Est. 1984

ORIENTAL JOURNAL OF CHEMISTRY

An International Open Access, Peer Reviewed Research Journal

www.orientjchem.org

ISSN: 0970-020 X
CODEN: OJCHEG
2023, Vol. 39, No.(3):
Pg. 684-693

Some Applications of CeO_2 Nanoparticles

KOMAL HUDDA[2], BARKHA RATHEE[1], MUKHAN WATI[1]*, SWEETY RANGA[1] and RAJDEEP TYAGI[2]

[1]Department of Chemistry, Maharshi Dayanand University, Rohtak-124001, Haryana, India.
[2]Department of Chemistry, University of Delhi, New Delhi-110007, India.
*Corresponding author Email-mukhandagar.rp.chem@mdurohtak.ac.in

http://dx.doi.org/10.13005/ojc/390319

(Received: February 16, 2023; Accepted: May 04, 2023)

ABSTRACT

Various properties of cerium oxide (Ceria, CeO_2) have been widely used in recent times. This article aims at discussing some fundamental properties of ceria, its application due to oxygen vacancies in its structure, its effects due to nano-size, synthesis strategy to give it a structure with diverse applications. Some basic applications of ceria-based structure have been reviewed. Ceria nanoparticles are used in catalytic converters in the automotive industries to convert harmful carbon monoxide to less harmful carbon dioxide, semiconductor industries uses it as fine abrasive and polishing agent, it can light production in mantles of gas lanterns where cerium oxide generates a yellowish white colour. Certain probable toxic effects and challenges in controllable synthesis of nanomaterials for its applications have been reviewed.

Keywords: Cerium dioxide, Nanoparticles, Techniques, Applications.

INTRODUCTION

Nanoparticles have size ranging between 1 to 100 nanometers. Nanotechnology is the science, which deals with the ability to control and manipulate matter nanoscale. At nanoscale, the properties change as compared to the bulk matter. This is due to two reasons.

Large surface area to volume ratio: As particle size gets smaller, more number of particles will be present on the surface than the bulk.Therefore, the ratio of surface area to volume increases many times in nanoparticles when compared to bulk matter. As the growth and catalysis of a reaction is dependent on surface, nanoparticles prove to be efficient and faster catalysts.

Dominance of quantum effect: As the particle size reduces to nanoscale, quantum effects start dominating. This changes the optical, magnetic and electrical properties of the matter[1].

Types of nanoparticles

Four types of nanoparticlesbased on sources used are:

Metallic nanoparticles: These Nano sized

metals have dimensions ranging from 1 to 100nm and high surface area to volume ratio. They havelow number of coordination sites. Someexamples of metallic nanoparticles are Cu, Au, Ag, Zn, etc.

Polymeric nanoparticles: These are dispersion of solid particulate matter withsize in the range of 1-1000nm, used as drug delivery system. Synthesis of these nanoparticles is carried out using biocompatible and biodegradable polymers. Polymeric nanoparticles can be used for dissolving several drugs.

Carbon based nanostructures: Graphene, diamond, nanotube and nanofibres are included inthis type. They have high surface area which is helpful for the deposition of metaloxide nanoparticles and conducting material. Properties like small dimensions, high thermalconductivity, low resistivity and high chemical stability makes them of great use.

Metal oxide nanoparticles: A number of metals form oxide-based nanoparticles. Their structural geometriesreveal their metallic, semi-conductor or insulator character. Some common types of metal oxidenanoparticles include Fe_2O_3, NiO, ZnO, MgO, etc. They have high density and limited size ofedges on the surfacesites, making them unique in terms of physical and chemical properties[2].

Ceria and its properties

Cerium a rare earth metal of lanthanide series with atomic number 58 exists in the common oxidation states +3 and +4. Cerium dioxide (CeO_2), an eminent cerium compound is a yellow-white powder usually formed by the calcination of cerium hydroxide or oxalate. Cerium oxide is one of the most abundant and reactive element among the lanthanides oxides. As compared to the bulk, CeO_2 nanoparticles have unique characteristics due to their shape and size[3]. In bulk material cerium dioxide exist as CeO_2 and Ce_2O_3 with +4 and +3 oxidation states respectively.

The interconversion of +3 and +4 oxidation states of Ceria is facile making it a key component for three-way catalysts (TWC) used for making electrodes in solid oxide fuel cells, electrolytes and for reduction of the emissions like CO, NOx and hydrocarbons from automobile exhaust[4,5,6].

Due to easy conversion between +3 and +4 oxidation states of cerium, Ceria is used in making catalysts that can store and release oxygen under oxidizing and reducing conditions respectively. CeO_2 is used as a catalyst, as polishing agent, in ultraviolet absorbers, gas sensors etc. Nanoparticles of ceria plays crucial role in commercial aspect as they are used in manufacturing of cosmetic products and instruments of high technology. They are good oxide ion conductors making their use crucial in development of gas sensor electrodes and solid oxide fuel cells. Polymer coating of ceria nanoparticles with dextran makes them to exhibit antioxidant property by enhancing their stability, solubility in water and bio-compatibility[7].

Electronic and Crystal structure

Cerium is the second member of lanthanide series after Lanthanum but is the most reactive lanthanide. It is electropositive ion existing in +3 and +4 oxidation states.Ce^{4+} having electronic configuration $[Xe]4f^0$ is more stable than $Ce^{+3}[Xe]4f^1$ as it has empty f-orbital. Cerium exists as Ceria (CeO_2) and Cerium sesquioxide (Ce_2O_3)[8].

Ceria (CeO_2) having a face centered cubic fluorite structure and space group F_3m_3 is the most stable oxide. Cerium ions are occupied in alternate cube centres of the simple cubic oxygen lattice. Eight oxygen atoms surround each metal ion. Pure Ceria having a band gap of 5eV can transform the material in a good n-type semiconductor when embedded with crystal defects and impurities. CeO_2 is not a pure ionic compound as indicated by experimental and theoretical data. Measurements by optical reflectivity and photoelectron spectroscopy shows there is significant metal character in the oxide even after the hybridization of the metal, orbitals of oxygen and dominance of valence band by 2p character of oxygen. This leads to a formal charge of less than +4 on the metal cation and describing CeO_2 as an iono-covalent compound.

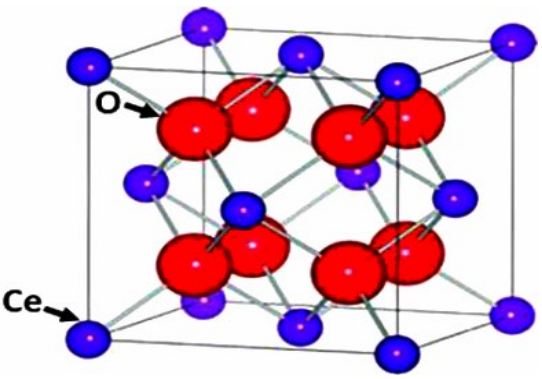

Fig. 1. Face centered cubic structure of ceria

Defects/Imperfections in bulk ceria

The ideal crystalline solid have a symmetrical arrangement of atoms. The crystal structure is a combination of a basic and infinite space lattice arranged periodically. As some atoms get displaced from their lattice positions it leads to imperfections in the crystal structure and breaks the perfect symmetry of the crystal. Crystal structure of Ceria has some extrinsic and intrinsic defects as well. Introduction of dopants and impurities are responsible for extrinsic defects. Thermal disorderness by oxidation reduction reactions between solid and surroundings, Schottkyand Frenkeldefects are common forms of intrinsic defects in the crystal[9].Reversible transition of +4 and +3 oxidation states of Cerium ions generate neutral oxygen vacancies leading to most stable and dominant form of defect in Ceria.

$$2ce^{4+} + O^{2-} \longrightarrow 2ce^{3+} + 1/2\ O_2$$

As an anionic oxygen (O^{2-}) leaves the lattice of Ceria, a neutral $1/2O_2$(g) species and two localized electrons trapped at two cerium sites are left behind. The electron at Cerium sites occupy empty 4f state which splitsinto two sub-bands: fully occupied Ce(4f) band and an empty Ce(4f) band.

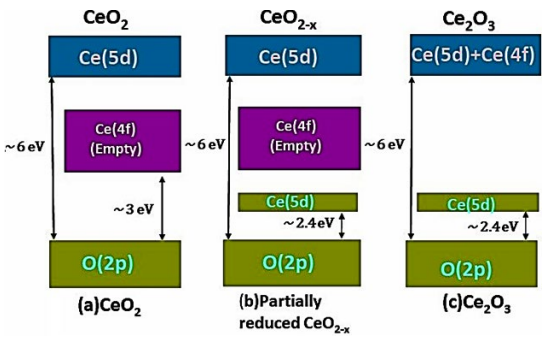

Fig. 2. Electronic structures of cerium oxides; green box depicts fully-occupied bands, blue and purple boxes represents empty bands

Non-stoichiometric ceria can be reduced to Ce_2O_3 practically, having all cerium ions in +3 oxidation state. Partially reduced ceria and Ce_2O_3 has resembling electronic band structure in which Ce 4f empty and Ce 5d bands are merged in the conduction band.

Oxygen vacancies in CeO_2

Replacement of cation sub-lattice of cerium oxide with lower valent elements creates higher deficiency of oxygen in the lattice resulting in increased oxygen ion conductivities. This property enhances its potential application as a solid electrolyte in fuel cells[10]. Low oxygen pressureand increased temperature releases oxygen, making it a mixed ionic electronic conductor. The ease with which ceria can occupy +3 and +4 oxidation states;small polarons(electrons) follows thermally mediated hopping mechanism in their lattice[11]. For improved transport and carrier properties,more mobile vacancies contributing to transport of oxygen ion in the solid solutions are considered.

Surface of CeO_2 nanocrystals have (100), (110) and (111) lattice planes, (111) plane have more exposed oxygen vacancies than (110) and (100) planes. In order to keep minimum surface energy nanoparticles possess octahedral and truncated octahedral shapes having most stable (111) facets. Minimum oxygen vacancies must be present on the surface ofnanocubes and nanorods. External factors such as doping, temperature can increase the concentration of oxygen vacancies in the crystal[12]. Higher concentration of oxygen vacancies on the surface favours redox reactions making ceria excellent for catalytic use.

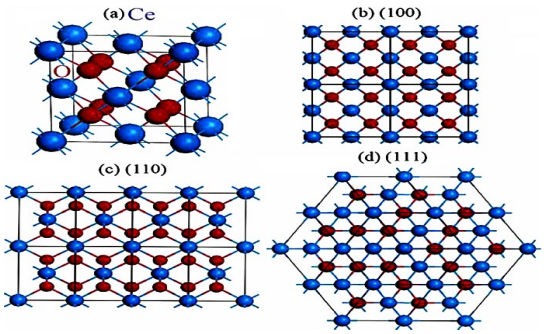

Fig. 3(a). Face-centred crystal cell of the CeO_2 structure; (b-d) (100) or (200), (110) and (111) planes of the CeO_2 structure

CeO_2 nanoparticles

Imperfections in nanoceria

In large nanoparticles, fluorite structure is observed whereas for small nanoparticles, amorphous structure is observed. A large deviation from the bulk fluorite structure is shown by the ceria nanoparticles. XRD, Raman, and XAS measurements suggestdistortions from the cubic fluoritestructure because of defects in the oxide lattice in little larger particles.As shown by XRD and Raman spectroscopy, preparation method

and oxidation state of Cerium in the precursor salt can change the number of oxygenvacancies and presence of Ce^{3+} ions in the crystal. Due to bigger size of Ce^{3+} ions than Ce^{4+} ions, higher oxygen vacancies leads to distorted unit cell. These increased oxygen vacancies and other surface effects introduces strain in the lattice and also gives it special electronic properties with electronic states lying within the band gap of the oxide. Ceria nanoparticles have considerably high conductivity than bulk particles[13].

Effects due to nano-size

A larger number of oxygen vacancies are created as the particle size is decreased in Ceria nano-particles. An increase in surface area to volume ratio of CeO_2 gives them unparalleled properties. Synthesis of CeO_2 nanoparticles of size 3-4nm supporting Au enhances the performance of catalyst for oxidation of CO by hundred times[14]. Size controlled tuning of CeO_2 nanoparticles can enhance its electronic conductivity, relaxation of lattice size and some other effects. Size of nanoparticles is very crucial as it leads to the expansion of lattice which in turn decreases its oxygen reabsorption and release capabilities.

Properties of CeO_2 nanoparticles

Crystal lattice of nanoparticles of Cerium oxide with cubic fluorite structure have Cerium in +3 as well as +4 oxidation states coexisting on its surface. Oxygen vacancies arecreated in the lattice for compensating charge deficiency; thus making CeO_2 nanoparticles to possess intrinsic oxygen defects. The intrinsic oxygen defects formed due to charge deficiency created by Ce^{3+} ions are potential sites of catalytic reactions. As particle size decreases, the concentration of defect increases. This leads to improved redox properties of cerium oxide nanoparticles than bulk. And the mixed valance states helps in scavenging of reactive nitrogen and oxygen species.The defects and oxygen vacancies in Ceria nanoparticles have electronic states lying within the bandgap of oxide introducing special electronic properties in them. Electronic conductivity of ceria nanoparticles is higher than bulk ceria. These can absorb and store hydrogen just as bulk ceria. As detected by XRD this absorption of hydrogen leads to expansion in the lattice constant of the cerium oxide. The absorbed hydrogen atoms move toward the oxygen sites forming hydroxyl species which act as the precursors for oxygen removal during a reduction process. XRD and temperature monitored reduction indicate that reduction temperatures of ceria nanoparticles are lower than those of bulk. The oxygen vacancies and embedded hydrogen leads to substantial expansion in the unit cell of the CeO_2 nanoparticle, before Ce_2O_3 appears in the reduction process. The high oxygen storage capacity and high oxygen mobility in the lattice provides biological application of ceria relevant to redox effect[15].

Classification of CeO_2 nanomaterials

Nanomaterials can be divided into four categories depending upon the number of dimensions[16]:

Zero dimension

All dimensions in nano range.

Examples: nanolanses, heterogeneous particles arrays, hollow spheres, quantum dots, and core-shell quantum dots.

One dimension

Two dimensions in nano range

Examples: nanowires, nanorods, nanotubes, nanobelts, nanoribbons.

Two dimension

One dimension in nano range

Examples: nanoplates, nanosheets, nanowalls.

Three dimension

No dimension in nano range

Examples: nanoballs, anocoils, nanocones, nanopillers.

Applications

Ceria is technologically a crucial material as it has remarkable implementations in wide range of spheres. Few extensively known industrial applications of ceria are:-

Solid oxide fuel cells

Solid oxide fuel cells (SOFCs) have the capability to provide well-grounded and clean electricity with lower emissions of nitrogen and sulphur oxides, hydrocarbon pollutants and green-gases[17,18]. They make up to an ecological and thence very alluring class of fuel cells, with electricity, water (as a result of using H_2 as a fuel) and heat as the most often outputs. They are compatible with various

fuels even without being subjected CO poisoning. Use of ceria in SOFC is common at the following three places:-

(1). In few designs, Doped ceria is used as an electrolyte.
(2). As a barrier layer to cathodes for preventing their reaction with the YSZ electrolyte.
(3). At times CeO_2 is used as a catalyst in both the cathodes and the anodes[19,20].

Performance of the catalyst can further be improved by doping with bivalent and trivalent elements as it increased the conduct. Gd-doped ceria anode (CGO) is a typical example in which the performance of the cell is enhanced as a result of the increase in the concentration of oxygen vacancies caused by the doping[21]. Ceria-based conductors are highly resistant to carbon deposition and have the capability to enable irresistible delivery fuels in the form of dry hydrocarbons to the Anode. The electrochemical oxidation of hydrocarbons, like methane and toluene using SOFC consisting of Ceria and Copper at temperature 1073K and 973K[22]. The design of Anode was Cu/CeO_2/YSZ, where Cu was mainly used as the current collector and CeO_2 as a catalyst for the oxidation reactions. These anodes are stable to redox reactions and their Sulphur tolerance is high upto 400ppm of Sulphur level without significant performance degradation.

Three way catalysts (TWCs)

The aim of the TWCs is to get rid of the pollutants generated during the combustion of gasoline and promoting oxidation of CO and unburnt hydrocarbons. They help in reducing nitrogen oxides (NO_x). A non-noble metal oxide promoter Pt-Pd-Rh supported over alumina was used to improve the performance of CO removal under oxygen deficient conditions. But CeO_2 acted as an oxygen buffer, thereby expanding the TWC's three-sided "window" of operation[23]. Reduced ceria (CeO_{2-y}) stores Oxygen while promoting the reduction of NO_x. Moreover, CeO_2 is capable of supplying the necessary oxygen for the oxidation of CO and HC in all transients. Recently the efficient control of pollutant emission is found out via modern TWCs prefers using pure CeO_2 instead of thesolid solution of CeO_2-ZrO_2 which were more resistant to sintering than naked CeO_2. Additionally, in the stable $CeAlO_3$ the undesirable fixation of Ce(III) is hindered[24].

Catalytic applications

The transition between +3 and +4 oxidation states alongwith their oxygen uptake makes ceria very useful for catalytic reactions. Recently, many nano micro ceria structures are developed to study their catalytic applications and oxidation of carbon monoxide being the maximum completely studied in it. At lower temperature, ceria nanomaterials increases the oxygen storage capability of catalysts. In general, nanomaterials which occupy high surface area are thought-about perfect for this application. The oxidation performance of CO can be judged by various recently presented reports discussing several morphologies. For example, the inner and outer surface in nanotubes,enhanced the performance of catalyst in CO oxidation by providing active sites for the adsorption of the reactant[25]. In contrast to the higher surface area and lower catalytic performance of the nanosized particles, the nanorods having larger diameter and lower surface area were found to be additionally active in CO oxidation[26,27].

Reduction of heavily discharged CO_2 into hydrocarbon fuels like CO, methane and methanol can be carried out using CeO_2 having advantaged of oxygen non-stoichiometry, high oxygen diffusion and controlled band gaps[28].

Diesel engines

Major pollutants like soot emitted from diesel engines, NO_x, CO and unburned hydrocarbons has proven negative impact on human health. Various methods have been introduced to decrease the amount of soot emitted, with catalytic filters as one of the most practised method. It involves filtering of the particulates followed by their catalytic oxidation. Drawbacks of this method involves the use of stable and active catalyst over a wide range of temperature, complexity in regeneration of filter and low efficiency of the catalyst.

For soot combustion, ceria is considered to be one of the best catalyst. For the soot combustion catalyst involving ceria, two majorily followed mechanisms are:

(1). Direct exchange of oxygen between the gas-phase O_2 and the catalyst in active oxygen mechanism.
(2). Oxidation of NO to NO_2 at higher temperature in NO_2 mechanism.

Bueno-Lopez *et al.,* published, mixed oxides of $Ce_{0.73}$-x$Zr_{0.27}Nd_xO_2$ with x ranging from 0 to 0.3 acts asan active catalyst for the oxidation of soot, propylene, CO and benzene simultaneously from a diesel exhaust mixture. Neodymium, when present in small quantities, results in higher performance due to reduced surface area and formation of oxygen vacancies. However when it is found in quantity more than 0.2, the final performance deteriorated as a result of sintering and reduced surface area. Control of CeO_2 in the nanorange can enhance the catalytic performance. It was recently reported that, $Co3O_4$ deposited CeO_2 nanocubesare outstanding catalysts[29,30].

Photocatalysis

Cation doping of oxide semiconductors not only modifies the phase and structure but also changes oxygen vacancy concentration[31]. Photocatalytic splitting of water in visible light is a research topic for renewable energy, air and water purification. Novel and efficient photocatalyst based on Au- supported CeO_2 nanoparticles have been prepared and Primo *et al.,* reported their activities in visible lights[32,33]. 1% w/w Au-supported ceria nanoparticles generated oxygen efficiently from water than tungsten oxide on irradiation with visible light of wavelength>400nm[34].

Ultrasmall ceria nanocubes have been synthesized. The consequence of indium doping was studied on the photocatalytic activity. On increasing the concentration of Indium doping,the photocatalytic activities build up to a certain extent. The photocatalytic activities were suppressed after this doping concentration because of the presence of In^{3+}. In^{3+} is capable of electron accepting and electron donating properties simultaneously. This causes the enlargement of electron-hole pair separation by capturing them near the valance and conduction bands[35].

Organic reactions

Nanoceria has been used as a stimulant in various organic reactions. A few examples include oxidation of p-Xylene, benzyl alcohol and p-chlorobenzyl alcohol etc.

Oxidation of para-xylene to terephthalic acid

Terephthalic acid is used to manufacture polyesters. The conventional method uses ethylene glycol, which in turn produces polyethylene terephthalate (PET). The PET is then used for making containers, packaging material and many more useful day-to-day things.

Commercially, terephthalic acid is prepared by aerobic oxidation of p-xylene in acetic acid but this reaction requires bromide-promoted heterogeneous catalyst which comprises of cobalt acetate and HBr under temperature ranging from 150–220°C and around 25bar.

But bromide promoter may corrode the titanium reactor and form bromomethane as a by-product, which is hazardous to environment. CeO_2 nanocrystals having a controlled size and morphology possessing large surface area and having exposed crystal planes have been used as an environment-friendly alternative for the same reaction.

$$C_6H_4(CH_3)_2 + 3O_2 \longrightarrow C_6H_4(COOH)_2 + 2H_2O$$

The nanocrystalline form has more defects than the bulk matter due to increased oxygen vacancies. This increases the catalytic activity of CeO_2 nanoparticles. It is assumed that the reaction occurs via a free radical chain mechanism. Primarily the reaction occurs on the exposed ceria surface.

$$2\ Ce(IV) + 2\ PhCH_3 \longrightarrow 2\ Ce(III)\text{-}PhCH_3^{+\cdot} \quad \text{(Initiation step)} \qquad (a)$$

$$2\ Ce(III)\text{-}PhCH_3^{+\cdot} + 2O_2 \longrightarrow 2\ Ce(IV) + 2\ PhCH_2O^{\cdot} + H_2O \qquad (b)$$

$$PhCH_2O^{\cdot} + PhCH_3 \longrightarrow PhCH_2OH + PhCH_2 \quad \text{(Propagation)} \qquad (c)$$

$$2\ PhCH_2OO^{\cdot} \longrightarrow PhCH_2OH + PhCHO + O_2 \quad \text{(Termination)} \qquad (d)$$

The reaction initiates with the adduct formation between para-xylene ($PhCH_3$) and the active sites of ceria followed by arylalkoxyl radical.

Arylalkoxyl radical is formed by the reaction of ceria(III) with $PhCH^{3+}$. Highly reactive arylalkoxyl radical then forms arylalkyl radical ($PhCH_2$.) by abstraction of H. Then radical gets oxygenated to form peroxyl radical ($PhCH_2OO$.). Thus,

self-reduction of exposed ceria leads to formation of the free radical from para-xylene[36].

Oxidation of benzyl alcohol, para-chlorobenzyl alcohol and toluene to the corresponding aldehyde

Commercially, benzaldehyde is synthesized by the incomplete oxidation of benzyl alcohol, oxidation of toluene in liquid phase and the carbonylation of benzene. The vital shortcomings in these methods of synthesis are caused because of the use of base additives, which result in formation of carboxylate products. The oxidation of benzyl alcohol in gaseous medium to its aldehyde is another method of synthesis. The over-oxidation of the products and the significant carbon loss in the form of CO_2 are the main difficulties in these processes.

CeO_2 nanocubes can be used as a catalyst for oxidation of benzyl alcohol in presence of air and toluene using molecular oxygen. Nanocubes could be used huge of times as a methodical and operative catalyst in producing benzaldehyde selectively[37].

Anti-bacterial activity

Bacterial contamination of wounds during treatment is the major contributor of morbidity and mortality. Fabricated nano-CeO_2 helps in healing of wound by enhancing tissue's antioxidant capacity, reducing bacterial count and accelerating proliferation of microblasts[38]. Nanoparticles of ceria show anti-bacterial activity against *Pseudomonas aeruginosa* through broth dilution method. At sufficient low temperature antibacterial activity was observed for *E. coli*, *Shewanella oneidensis*. The expected procedure was attributed to the activity of reactive oxygen species (ROS) which leads to bacterial cell death[39]. Nanoceria is active against both *Gram-positive* and *Gram-negative* bacteria via ROS generation but structural complexity of *Gram-negative* bacteria's membrane, makes it more sensitive against *Gram-positive* species[40,41].

Toxicity of nanoceria

Parameters

Cerium is not found in the human body and there are no clearance mechanisms for it. This implies cerium can cause severe toxicity[42]. High positive charge and small size of the ceria particles allows good electrostatic interactions leading to better penetration into the cell membrane causing toxicity[43]. Other factors on which toxicity of cerianano materials depends are modes of synthesis, nature of stabilizing agent used and percentage of Ce^{3+} and Ce^{4+} present on the surface.

Particle size

Several green methods have been used for the preparation of CeO_2- nanoparticles. Biopolymer and nutrient-based methods have been used to synthesize the smallest category of nanoparticles. These exhibit no harmful effects to human cells even at higher concentrations. Plant-based CeO_2-nanoparticles displayed antibacterial properties but at the cost of high levels of cytotoxicity to bacterial cells[44].

Morphology

Nanoparticles are capable of having different shapes such as polygonal, cuboidal or rod shaped. The sharp edges of these kind of shapes can harm the human cells therefore the shape of nanoparticles plays an important role in considering the toxicity of nanoceria. Majorily the green methods of ceria synthesis results in spherical nanoparticles. Starch-based synthesis CeO_2- nanoparticles are used for biomedical purposes[44].

Percentage of surface Ce^{3+}

It was found out that concentration, surface charge and size of CeO_2-nanoparticles do not play much important role in determining the toxic properties. The main cause of toxicity of CeO_2-nanoparticles is the percentage of surface Ce^{3+}. The nanoparticles with the maximum percentage of surface Ce^{3+} showed the most lethal effect and CeO_2-nanoparticles with lesser percentage of surface Ce^{3+} values (between 26% and 36%) turned out to be evidently non-toxic. In fact, nanoparticles with higher Ce^{4+} on their surface showed activity similar to that of catalase or peroxidase. CeO_2-nanoparticles with higher Ce^{3+} on their surface can hunt radicals of superoxide and in turn generate H_2O_2, which is dangerous to the cells[45].

Characterisation

UV-Visible spectra

CeO_2 nanoparticles are optically and photo-catalytically active (depends on its optical property), which is confirmed by the absorption band at 298nm in UV-Visible spectra. This peak correlates to the fluorite structure of CeO_2. As the particle size is decreased, the band gap will increase in semiconductors.

In the visible region, color changes with size. As the energy band gap increases, the nanoparticles exhibit blue shift in the UV-Visible region. This blue shift is a testimony of the existence of nanoparticles.

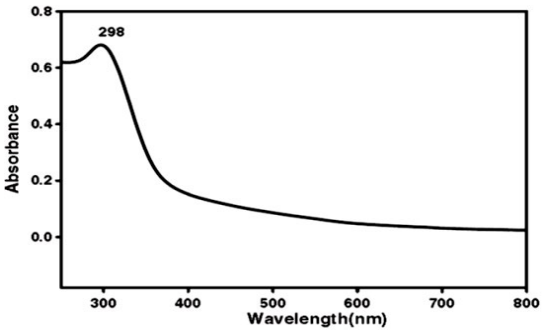

Fig. 8. UV–Visible spectrum of the synthesized CeO_2 nanoparticle

FTIR analysis

Four strong absorption peaks were observed at 3343, 1600, 1400 and 554 cm^{-1}.

- 3343 cm^{-1}: Stretching band of hydroxyl group`
- 1600 cm^{-1}: anti-symmetric stretching band
- 1400 cm^{-1}: Symmetric stretching band
- 554 cm^{-1}: Ce-O stretching vibration[46].

XRD analysis

Fluorite structure is possessed by CeO_2. In this type of structure Ce^{4+} is coordinated with eight equivalent O_2- ions. On the other hand, each O_2 is linked to four Ce^{4+} ions.

The CeO_2 nanoparticles are crystalline in nature. The nanoparticles possess face centered cubic structure (FCC). The average size of a CeO2 nanoparticle was found to be 10nm.

In the face centered cubic (FCC) structure of ceria, Ce^{4+} ions were found to exist in a cubic close packing arrangement. The oxide ions occupied the tetrahedral sites and the octahedral sites remained unoccupied.

- The face centers and corners tend to be occupied by Ce^{4+} ions.
- The body center position was observed to be occupied by oxide ions[47,48].

Raman spectra

The excitation wavelength at 633nm corresponding to intrinsic oxygen vacancies in the Raman spectra indicates non-stoichiometry of nanocrystals of CeO_2[49]. The highest intensity peak is observed at 461.8 cm^{-1} due to symmetric stretching mode of Ce-O_8 unit. Along with this, two other low intensity peaks are also observed[50].

Scanning Electron Microscopy (SEM) analysis

SEM image for Ceria unveiled that there are various dimensions of particles in the given sample. The large particles consist of small embryonic crystals and exhibit particle clusters of non-uniform shapes and sizes (1-6 µm). The EDX suggests the existence of Ce and O. EDX measurements on every different spot of the sample always gave the identical patterns, which pointed towards the uniformity of the sample. Characterization of Ceria nanoparticles can be carried out using Field Emission Scanning Electron Microscopy. Generation of high resolution images with low acceleration voltages from sharp field emission gun made FESEM more reliable than SEM[51].

CONCLUSION

The major concern of nanoceria is how it impacts the health of humans. It was inferred that nanoceria turned out to be hazardous towards human cancer cell lines. The release of free radicals can result in destruction of the cell membrane and peroxidation of lipid. Ceria nanoparticles have turned out to be safer nanoparticles in vitro models as compared to *In vivo* models. By far CeO_2 nanoparticles are commercially used cerium compounds for electronics, automotive and solar panel for energy. CeO_2 nanoparticles have proved to be potential therapeutic agents. They have shown to have regenerative anti-oxidant properties. The properties of CeO_2 nanoparticles, such as size and charge on surface, exhibit pivotal role in the reciprocal action of the nanoparticles with the target cells. Exploiting biocompatible CeO_2 nanoparticles may enhance results deeply with innumerable applications in nanobiotechnology.

ACKNOWLEDGEMENT

I acknowledge all the co-authors and Maharshi Dayanand University for their constant support.

Conflict of interest

There is no conflict of interest.

REFERENCES

1. The Royal Society and The Royal Academy of Engineering Nanoscience and nanotechnologies, **2004**, Chapter 2 & 3;www.nanotec.org.uk/finalReport.htmISBN 0 85403 604 0.
2. Robert, T.; Sylvain, C.;Todd, O.;Patric, P.;Andrey, G.;Wei, L.; Gary, P.; Ravi;Himanshu, T. *J. Appl. Phy.*, **2013**, *113*, 011301. DOI:10.1063/1.4754271.
3. Deori, K.; Gupta, D.; Saha, B.; Deka, S. *ACS Catal.*, **2014**, *4*, 3169–3179. DOI: https://doi.org/10.1021/cs500644j.
4. Mittal, A.; Gupta, V. K.; Malviya, A.; Mittal, J. *J. Hazard Mater.*, **2008**, *151*, 821. DOI: https://doi.org/10.1016/j.jhazmat.2007.06.059.
5. Gupta, V.K.; Ali, I.; Saini, V. K. *J Colloid Interface Sci.*, **2007**, *87*, 315. DOI: 10.1016/j.jcis.2007.06.063.
6. Deshpande, S. S.;Sonavane, S. U.; Jayaram, R. V. *Cat. Com.*, **2008**, *9*, 639. DOI:10.1016/J.CATCOM.2007.06.023.
7. Dahle, J. T.; Arai, Y. *Int. J. Environ. Res. Public Health.*, **2015**, *12*, 1253–1278. DOI: 10.3390/ijerph120201253.
8. Malavasi, L.; Fisher, C.A.J.; Islam, M.S. *Chem. Soc. Rev.*, **2010**, *39*, 4370–4387. DOI:10.1039/b915141a.
9. Younis, A.; Chu, D.; Li, S.; Cerium Oxide Nanostructures and their Applications, Functionalized Nanomaterials, Dr. Muhammad Akhyar Farrukh (Ed.), *InTech.*, **2016**, chapter 3,DOI:10.5772/65937.
10. Guo, X.; Waser, R. *Prog. Mater. Sci.*, **2006**, *51*, 151–210. DOI:10.1016/J.PMATSCI.2005.07.001.
11. Tuller, H. L.; Nowick, A. S. *J. Phys. Chem. Solids.*, **1977**, *38*, 859–867. DOI:https://doi.org/10.1016/0022-3697(77)90124-X.
12. Campbell, C. T.; Peden, C. H. F. *Science.,* **2005**, *309*, 713–714. DOI: 10.1126/science.1113955.
13. Montini, T.; Melchionna, M.; Monai, M.; Fornasiero, P. *Chem. Rev.*, **2016**, *116*, 5987–6041. DOI: 10.1021/acs.chemrev.5b00603.
14. Carrettin, S.; Concepcion, P.; Corma, A.; Nieto, J. M. L.; Puntes, V. F. Angew. *Chem. Int. Ed.*, **2004**, *43*, 2538–2540. DOI:10.1002/ANIE.200353570.
15. Li, H.; Xia, P.; Pan, S.; Qi, Z.; Fu, C.; Yu, Z.; Kong, W.; Chang, Y.; Wang, K.; Wu, D.; Yang, X. *Int. J. Med.*, **2020**, *15*, 7199-7214. DOI: 10.2147/IJN.S270229.
16. Tiwari, J. N.; Tiwari, R. N.; Kim, K. S. *Prog. Mater. Sci.*, **2012**, *57*, 724–803. DOI: https://doi.org/10.1016/j.pmatsci.2011.08.003.
17. Alder, S. B. *Chem. Rev.*, **2004**, *104*, 4791. DOI: https://doi.org/10.1021/cr020724o.
18. Ormerod, R. M. *Chem. Soc. Rev.*, **2003**, *32*, 17. DOI:https://doi.org/10.1039/B105764M.
19. Takahashi, T.; Physics of Electrolytes; Hladik, J., Ed.; Academic Press: London, **1972**, 291 DOI: https://doi.org/10.1038/248713b0.
20. Mogensen, M. *J. Electrochem. Soc.*, **1994**, *141*, 2122–2128. DOI: 10.1149/1.2055072.
21. Marina, O. A.; Bagger, C.; Primdahl, S.; Mogensen, M. *Solid State Ion.*, **1999**, *123*, 199–208. DOI:10.1016/S0167-2738(99) 00111-3.
22. Gorte, R.J.; Vohs, J. M. *Curr. Opin. Colloid Interface Sci.*, **2009**, *14*, 236–244. DOI: https://doi.org/10.1016/j.cocis.2009.04.006.
23. Kim, G.; *Ind. Eng. Chem. Prod. Res. Dev.*, **1982**, *21*, 267-274. DOI: https://doi.org/10.1021/i300006a014.
24. Wang, Z. L.; Feng, X. D. *J. Phy. Chem. B.*, **2003**, *107*, 13563-13566. DOI: https://doi.org/10.1021/jp036815m.
25. Montini, T.; Melchionna, M.; Monai, M.; Fornasiero, P. *Chem. Rev.*, **2016**, *116*, 5987–6041. DOI: 10.1021/acs.chemrev.5b00603.
26. Pan, C. S.; Zhang, D. S.; Shi, L.Y. *J. Solid State Chem.*, **2008**, *181*, 1298–1306. DOI: 10.1016/j.jssc.2008.02.011.
27. Tana; Zhang, M.; Li, J.; Li, H.; Li, Y.; Shen, W. *Catal. Today.*, **2009**, *148*, 179–183 DOI: 10.1016/j.cattod.2009.02.016.
28. Zhang, D. S.; Niu, F. H.; Yan, T. T.; Shi, L.Y.; Du, X.J.; Fang, J. H. *Appl. Surf. Sci.*, **2011**, *257*, 10161–10167. DOI: https://doi.org/10.1016/j.apsusc.2011.07.010.
29. Ma, Y.; Gao, W.; Zhang, Z.; Zhang, S.; Tian, Z.; Liu, Y.; Ho, J., C.; Qu, Y. *Surf. Sci. Rep.*, **2018**, *73*, 1-36. DOI: 10.12691/jap-7-1-1.
30. Ciambelli, P.; Palma, V.; Russo, P.; Vaccaro, S. *Catal. Today.*, **2002**, *75*, 471–478. DOI: https://doi.org/10.1016/S0920-5861(02)00098-6.
31. Younis, A.; Chu, D.; Kaneti, Y.V.; Li, S. *Nanoscale.*, **2016**, *8*, 378–387. DOI: https://doi.org/10.1039/C5NR06588G.

32. Santos Xavier, L. P.; Rico-Pérez, V.; Hernández-Giménez, A. M.; Lozano-Castelló,D.; Bueno-López, A. *Appl. Catal.*, B. **2015**, *216*, 412–419. DOI: https://doi.org/10.1016/j.apcatb.2014.07.013.
33. Bueno-López, A. *Appl. Catal. B.*, **2014**, *146*, 1–11. DOI: https://doi.org/10.1016/j.apcatb.2013.02.033.
34. Primo, A.; Marino, T.; Corma, A.; Molinari, R.; Garcia, H. *J. Am. Chem. Soc.*, **2011**, *133*, 6930–6933. DOI: 10.1021/ja2011498.
35. Tang, Z.; Zhang, Y.; Xu, Y. *RSC Advances.*, **2011**, *1*, 1772–1777. DOI:10.1039/C1RA 00518A.
36. Deori, K.; Gupta, D.; Saha, B.; Awasthiand, K. S.; Deka, S. *J. Mater. Chem. A.*, **2013**, *1*, 7091–7099. DOI: 10.1039/c3ta01590d.
37. Deori, K.; Kalita, C.; Deka, S. *J. Mater. Chem. A.*, **2015**, *3*, 6909–6920. DOI: 10.1039/C4TA 06547F.
38. Charbgoo, F.; Ahmad, M. B.; Darroudi, M. *Int. J. Nanomedicine.*, **2017**, *12*, 1401–1413. http://dx.doi.org/10.2147/IJN.S124855.
39. Shcherbakov, A. B.; Reukov, V. V.; Yakimansky, A. V.; Krasnopeeva, E. L.; Ivanova, O. S.; Popov, A. L.; Ivanov, V. K. *Polymers.*, **2021**, *13*, 924. DOI: 10.3390/polym13060924.
40. Singh, K. R. B.; Sridevi, P.; Singh, R. P.; Authorea, preprint, **2019**, 10.22541/au.157773086.64212371. DOI:10.1002/eng2.12238.
41. Nadeem, M.; Khan, R.; Afridi, K.; Nadhman, A.; Ullah, S.; Faisal, S.; Mabood, Z. U.; Hano, C.; Abbasi, B. H. *Int. J. Nanomedicine.*, **2020**, 5951-5961. DOI: https://doi.org/10.2147/IJN.S255784.
42. Thakur, N.; Manna, P.; Das, J. *J. Nano-biotechnology.*, **2019**, *84*. DOI:10.1186/s12951-019-0516-9.
43. Khan, M.; Mashwani, Z.-u.-R.; Ikram, M.; Raja, N.I.; Mohamed, A. H.; Ren, G.; Omar, A. A. *Nanomaterials.*, **2022**, *12*, 2117. DOI: 10.3390/nano12122117.
44. Carboo F.; Ahmed B., M.; Darroudi M. *Int. J. Nano Medicine.*, **2017**, *12*, 1401-1413.
45. Xu, C.; Qu, X. *NPG Asia Mater.*, **2014**, *6*, 90. DOI: 10.1038/am.2013.88.
46. Khan, S. B.; Faisal, M.; Rahman, M. M.; Jamal, A. *Sci. Total Environ.*, **2011**, *409*, 2987 2992. https://doi.org/10.1016/j.scitotenv.2011.04.019.
47. Rao, G. G.; Mishra, B. G. Bul. Cat. Soc. Ind., **2003**, *2*, 122.
48. Wang, G.; Mu, Q.; Chen, T.; Wang, Y. *J. Alloys Compd.*, **2010**, *493*, 202–207. https://doi.org/10.1016/j.jallcom.2009.12.053.
49. Kostic, R.; Askrabic, S.; Dohcevic-Mitrovic, Z.; Popovic, Z., V. *Appl. Phys. A.*, **2008**, *90*, 679-683. DOI:10.1007/s00339-007-4345-6.
50. Rajesh Kumar, S.; Naik, P. *Biotechnology Reports.*, **2018**, *17*, 1–5, DOI: https://doi.org/10.1016/j.btre.2017.11.008.
51. Mutalib, M. A.; Rahman, M. A.; Oathman, M. H. D.; Ismail, A. F.; Jaafar, J. Scanning Electron Microscopy (SEM) and Energy-Dispersive X-ray (EDX) Spectroscopy. In Membrane Characterization; Elsevier B. V.: Amsterdam, The Netherlands, **2017**; Chapter 9 ISBN 9780444637765. DOI: 10.1016/B978-0-444-63776-5.00009-7.